Tuning the relaxation behaviour by changing the content of cobalt in $Co_xFe_{3-x}O_4$ ferrofluids

2005 J. Phys.: Condens. Matter 17 7875

(http://iopscience.iop.org/0953-8984/17/50/008)

INSTITUTE OF PHYSICS PUBLISHING JOURNAL OF PHYSICS: CONDENSED MATTER

J. Phys.: Condens. Matter **17** (2005) 7875–7883 doi:10.1088/0953-8984/17/50/008

Tuning the relaxation behaviour by changing the content of cobalt in $Co_xFe_{3-x}O_4$ ferrofluids

Birgit Fischer, Joachim Wagner, Michael Schmitt and Rolf Hempelmann[1]

Physical Chemistry, Saarland University, 66123 Saarbrücken, Germany

E-mail: R.Hempelmann@mx.uni-saarland.de

Received 9 August 2005, in final form 5 October 2005
Published 2 December 2005
Online at stacks.iop.org/JPhysCM/17/7875

Abstract

The frequency-dependent magnetic relaxation of $Co_xFe_{3-x}O_4$ nanoparticles stabilized by *N*-methyloleamidoacetic acid is investigated in three apolar suspending media (toluene, cyclohexane and decane). Hereby, the dependence of the crossover from a Brownian to a Néelian relaxation mechanism on the cobalt content is observed. The experimental results obtained from the complex magnetic susceptibility confirm the theoretically expected crossover between both relaxation mechanisms. The topological characterization is performed by means of x-ray diffraction, photon correlation spectroscopy and—in the Brownian regime—by magnetic relaxometry, allowing the comparison of crystallographic and hydrodynamic particle sizes.

1. Introduction

Due to the variety of both technical (i.e. rotating shaft sealings) and biomedical applications (i.e. hyperthermia, magnetic drug delivery), ferrofluids have induced a large interest in fundamental and applied research during recent years [1–3]. The macroscopic properties of these magnetic suspensions depend on the mesoscale structure and on the magnetic properties of the suspended particles. The magnetism of such nanoparticles strongly depends on the particle topology. Thus, in addition to the chemical composition of the particles, their shape, size and even size distribution can be used to tune the macroscopic magnetic properties. Within this contribution, we investigate the influence of the composition of a mixed ferrite system on the magnetism of nanoparticles: in most cases, the composition can be varied much more easily than the topology.

[1] Author to whom any correspondence should be addressed.

0953-8984/05/507875+09$30.00

2. Theoretical background

The magnetism of nanoparticles can be characterized by the relaxation behaviour. There are two distinct mechanisms known for the magnetic relaxation of nanoparticles. Either the whole particle rotates within the carrier liquid with its magnetic moment locked in an easy direction of magnetization (so-called Brownian relaxation), or by spin flip processes only the magnetic moment rotates within the stationary particle (so-called Néel relaxation) [4]. The faster of these two possible processes determines the magnetic relaxation behaviour. The essential quantity which determines the velocity of spin flipping is the magnetic anisotropy. This energy $E = K V_{\mathrm{mag}}$ with the anisotropy constant K is proportional to the particle volume V_{mag}. For materials with sufficiently large anisotropy constant K, so-called hard magnetic materials, the rotation of the whole particle can be faster than a spin flip in the lattice. Hence, the magnetization of those particles relaxes via a rotational diffusion process characterized by the rotational diffusion coefficient that can, for a sphere with diameter D_{hyd} immersed in a carrier liquid with the viscosity η, be expressed as

$$D_{\mathrm{rot}} = \frac{k_{\mathrm{B}} T}{\pi \eta D_{\mathrm{hyd}}^3}. \tag{1}$$

Here D_{rot} is the Einstein rotational diffusion coefficient for single particle. The characteristic relaxation time according to this Brownian mechanism is

$$\tau_{\mathrm{B}} = \frac{1}{l(l+1) D_{\mathrm{rot}}} = \frac{\pi D_{\mathrm{hyd}}^3}{2 k_{\mathrm{B}} T} \eta \tag{2}$$

with $l = 1$ denoting the tensor rank of the quantity observed, i.e. the magnetic moment. The mixed ferrites $A_x B_{3-x} O_4$ can be described by the spinel structure. Depending on the cations involved, a gradual change to an inverse spinel is possible. The classical ferrite Fe_3O_4, with $K = -11$ kJ m^{-3}, is a soft magnetic material [5]. In contrast, cobalt ferrite $CoFe_2O_4$ with $K = 200$ kJ m^{-3} is a hard magnetic material [5]. The sign of K is just an indicator for the relative orientation of the preferred direction of magnetization towards the lattice orientation. Soft magnetic materials show a small remanent magnetization. As a consequence, the use of such materials in the construction of transformers can minimize losses due to hysteresis. In contrast, the large remanence of hard magnetic materials is essential for permanent magnets. Recently, Ayala-Valenzuela *et al* have shown the possibility to gradually change K by variation of the mixed ferrite stoichiometry $Co_x Fe_{3-x} O_4$ [6].

The critical quantity that determines the mechanism of magnetic relaxation is the magnetic anisotropy energy $K V_{\mathrm{mag}}$. If this energy is significantly larger than the thermal energy $k_{\mathrm{B}} T$, Brownian relaxation will take place. In the opposite case $K V_{\mathrm{mag}} \ll k_{\mathrm{B}} T$, the Néel process is faster and will dominate. For $CoFe_2O_4$ the critical volume V_{mag} is already exceeded for particles with a diameter $D_{\mathrm{mag}} > 5$ nm. In the case of the soft magnetic Fe_3O_4, however, particles with a diameter $D_{\mathrm{mag}} > 9$ nm are required for a Brownian relaxation. In a recent study [7], we have shown the linear dependence of the Brownian relaxation time on the viscosity and how to derive the hydrodynamic diameter distribution from the relaxation time for polydisperse systems. In the Néelian regime, the relaxation time could be calculated according to [8, 9]

$$\tau_{\mathrm{N}} = \tau_0 \exp\left(\frac{K V_{\mathrm{mag}}}{k_{\mathrm{B}} T}\right), \qquad \text{for} \quad \frac{K V_{\mathrm{mag}}}{k_{\mathrm{B}} T} \ll 1. \tag{3}$$

The extinction time τ_0 can be approximated to 10^{-9} s [10].

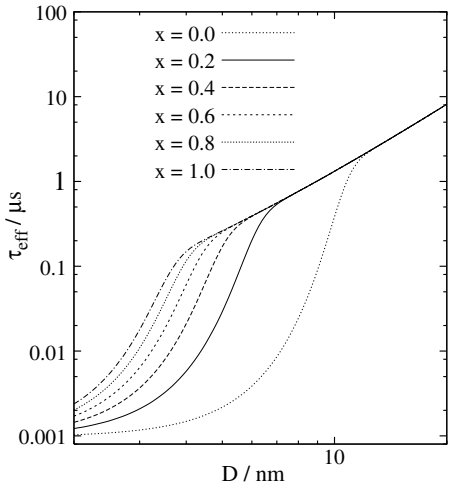

Figure 1. Relaxation time for $Co_xFe_{3-x}O_4$ with ($x = 0, 0.2, \ldots, 1$) calculated according to equation (4) versus the particle diameter.

A distribution of particle sizes implies a spectrum of relaxation times with contributions from both mechanisms. As a consequence, the effective relaxation time τ_{eff} is given by the median [11]

$$\tau_{\text{eff}} = \frac{\tau_{\text{B}}\tau_n}{\tau_{\text{B}} + \tau_{\text{N}}}. \tag{4}$$

The calculation of the relaxation time has a high uncertainty, because of the approximation of τ_0 and K [12]. In figure 1 the relaxation time versus the particle diameter for magnetite and cobalt ferrite are displayed according to equation (4).

Particles produced by the precipitation method are in a range of diameters between 5 and 15 nm. From figure 1 it can easily be seen that cobalt ferrite particles of this size relax according to a Brownian mechanism, whereas for magnetite a pure Néelian mechanism has to be expected.

By variation of the molar ratio of the two-valent iron and cobalt precursor, the stoichiometry of the mixed ferrite $Co_xFe_{3-x}O_4$ can be tuned. Assuming in a first attempt a linear dependence of the anisotropy constant on the stoichiometry, a gradual transition from Brownian to Néelian relaxation can be expected with increasing iron content. As a consequence the apparent effective relaxation time should change with the cobalt content.

In figure 1 the dependence of the effective relaxation time on the cobalt content is displayed. Hereby, the anisotropy constant is estimated by a linear interpolation between pure cobalt ferrite ($x = 1$) and pure magnetite ($x = 0$).

Experimentally, the relaxation time is accessible from the complex magnetic susceptibility as a function of the frequency f.

For a monodisperse system of non-interacting rigid dipoles suspended in a liquid carrier, a Debye relaxation according to [13]

$$\chi(f) = \frac{\chi_0}{1 + 2\pi \mathrm{i} f \tau_{\text{B}}} \tag{5}$$

with the static susceptibility

$$\chi_0 = \frac{N}{V}\frac{\mu_0 m^2}{k_{\text{B}}T} \tag{6}$$

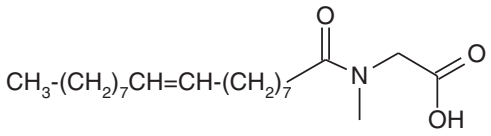

Figure 2. Structure of *N*-methyloleamidoacetic acid.

will occur. N/V denotes the number density of the spherical particles, and m the magnetic moment of one single-domain particle given by

$$m = M_s \frac{\pi}{6} D_{\mathrm{mag}}^3. \tag{7}$$

Here, D_{mag} is the diameter of the magnetic core of the particle. The thickness of the nonmagnetic layer consisting of a magnetic dead layer and the surfactant is described by δ. The apparent hydrodynamic diameter D_{hyd} is

$$D_{\mathrm{hyd}} = D_{\mathrm{mag}} + 2\delta. \tag{8}$$

In the case of the sterically stabilized ferrofluids, δ can be correlated to the length of the surfactant molecules.

Real ferrofluids, however, are polydisperse. Therefore, for each particle size in the system, a corresponding Debye relaxation contributes to the whole spectrum, weighted by the relative number of particles at the given sizes. Hence

$$\frac{\chi(f)}{\chi_0} = \frac{1}{\langle (D_{\mathrm{hyd}} - 2\delta)^6 \rangle} \int_{2\delta}^{\infty} \frac{(D_{\mathrm{hyd}} - 2\delta)^6}{1 + 2\pi \mathrm{i} f \tau_{\mathrm{B}}} F(D_{\mathrm{hyd}})\, \mathrm{d}D_{\mathrm{hyd}}. \tag{9}$$

$F(D_{\mathrm{hyd}})$ is a distribution function assumed to be of Schulz–Flory type:

$$F_{\mathrm{SF}} = \frac{1}{z!} \left(\frac{z+1}{D_0} \right)^{z+1} D^z \exp\left(-\frac{z+1}{D_0} D \right) \tag{10}$$

with the median diameter D_0 and the polydispersity P:

$$P = \left(\frac{\langle D^2 \rangle - \langle D \rangle^2}{\langle D \rangle^2} \right)^{\frac{1}{2}} = \left(\frac{1}{z+1} \right)^{\frac{1}{2}}. \tag{11}$$

3. Experimental details

The $Co_xFe_{3-x}O_4$ is prepared by a coprecipitation starting from the solution of the precursors $CoCl_2$ and $FeCl_2$ (x:$(1-x)$) and $FeCl_3$ with a surplus of NaOH. For the sterical stabilization of the ferrofluid the surfactant *N*-methyloleamidoacetic acid ($C_{21}H_{39}NO_3$), see figure 2, is used. The mixture of the magnetic particles and *N*-methyloleamidoacetic acid in water is heated to 80 °C for 1 h. By adding a small amount of hydrochloric acid, the precipitate agglomerates and can be separated from the liquid. The resulting slurry is washed in order to remove the salts and redispersed in decane, toluene or cyclohexane, respectively, acting as apolar dispersion media with different viscosities.

For the ac-susceptibility measurements, a Solatron 1260 impedance analyser is used. In this, magnetic fluid with a magnetic volume fraction ϕ of about 0.005 is inserted in an inductive coil; the changes of its inductance are analysed in a frequency range between 100 Hz and 500 kHz. For the dynamic light scattering (DLS) experiments a goniometer system purchased from ALV, Langen, Germany with a HeNe laser of 35 mW (Coherent) is used.

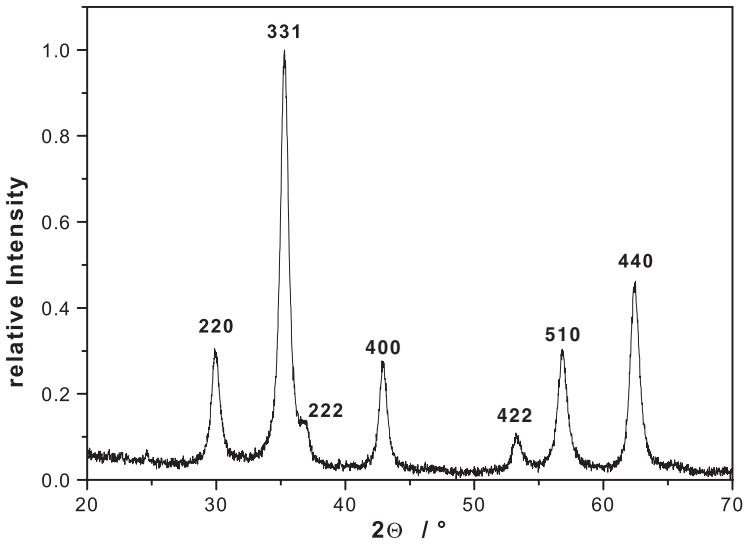

Figure 3. Typical x-ray diffraction pattern for the coprecipitated powder of the $Co_xFe_{3-x}O_4$ system, where $x = 0.5$.

Table 1. Diameter medians and polydispersity of the magnetic particles as obtained from the x-ray diffractometry, for different cobalt contents x in $Co_xFe_{3-x}O_4$.

x	0.0	0.1	0.2	0.3	0.4	0.5	0.6	0.7	0.8	0.9	1.0
$D_{0,\mathrm{mag}}$ (nm)	10.5	8.6	10.0	9.6	7.7	9.6	7.3	12.4	7.3	7.5	8.2
P	0.23	0.11	0.18	0.18	0.38	0.29	0.43	0.34	0.50	0.43	0.23

Table 2. Hydrodynamic diameter medians and polydispersity as determined by DLS for $Co_xFe_{3-x}O_4$ with $x = 0.1, 0.2, 0.3, 0.4$.

	Toluene		Decane		Cyclohexane	
x	$D_{0,\mathrm{hyd}}$ (nm)	P	$D_{0,\mathrm{hyd}}$ (nm)	P	$D_{0,\mathrm{hyd}}$ (nm)	P
0.1	35	0.29	48	0.17	51	0.27
0.2	43	0.20	66	0.18	44	0.17
0.3	43	0.17	57	0.33	51	0.17
0.4	58	0.39	41	0.27	22	0.21

4. Results

The characterization of the crystallite size is done by line shape analysis of the x-ray diffraction pattern resulting from the dry magnetic powder.

A typical diffractogram for such a spinel structure is displayed in figure 3. The particle size distribution is obtained by analysis of the two harmonic reflections 220 and 440 according to the Warren–Averbach method [14, 15]. We get distribution functions with median diameters between 7.5 and 10.5 nm and a polydispersity between 0.11 and 0.50. The results are compiled in table 1.

The hydrodynamic diameters are determined by DLS using a sample diluted by a factor of 1000. The results obtained from the CONTIN algorithm are shown in table 2 [16].

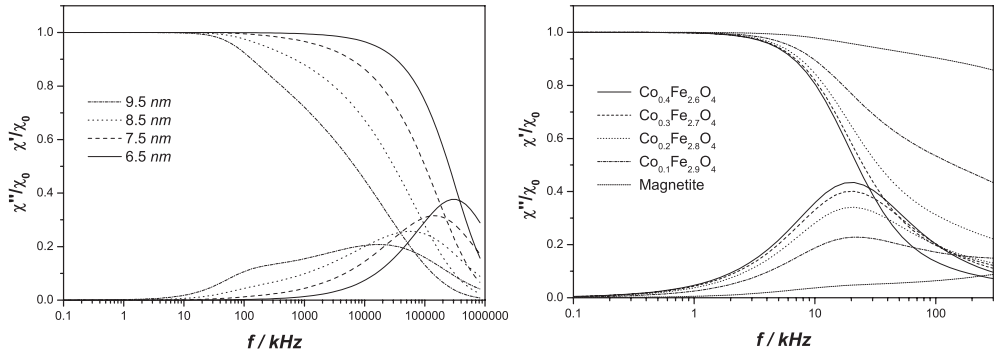

Figure 4. The ac-susceptibility calculated by equation (9) for magnetite (left) with $\delta = 2$ nm, $P = 0.18$ and $\eta = 1$ mPa s and for $Co_xFe_{3-x}O_4$ (right) with $D_0 = 7.5$ nm, $P = 0.27$ and $\eta = 1$ mPa s. The effective relaxation times are calculated according to equation (4).

Table 3. Absolute low-frequency limits χ at 1 kHz of the susceptibility for different cobalt contents x in $Co_xFe_{3-x}O_4$ in toluene (A), decane (B) and cyclohexane (C).

x	0.0	0.1	0.2	0.3	0.4	0.5	0.6	0.7	0.8	0.9	1.0
χ (1 kHz) A	0.07	0.13	0.02	0.01	0.07	0.07	0.03	0.02	0.05	0.02	0.18
χ (1 kHz) B	0.05	0.04	0.04	0.02	0.01	0.07	0.04	0.01	0.02	0.03	0.15
χ (1 kHz) C	0.06	0.05	0.04	0.04	0.02	0.05	0.08	0.04	0.10	0.02	0.02

Assuming a suitable particle size distribution, the complex magnetic susceptibility can be calculated according to equation (9). Here we assume a distribution with a polydispersity $P = 0.18$, a shell thickness $\delta = 2$ nm and a viscosity $\eta = 1$ mPa s. The calculated susceptibility data of magnetite with different medians are shown in figure 4 (on the left-hand side). It is evident that by variation of the particle diameter median the relaxation time can be varied.

Another possibility is given by changing the content of cobalt. In figure 4 (on the right-hand side) the ac-susceptibility for different contents of cobalt is displayed. For inverse spinels $Co_xFe_{3-x}O_4$ with $x > 0.5$, a Brownian relaxation is predominant, which solely depends on the hydrodynamic particle volume in the fluid and the viscosity of the dispersion medium.

In figure 5 the complex magnetic susceptibility of $Co_xFe_{3-x}O_4$ with *N*-methyloleamidoacetic acid in the three different solvents is displayed. The absolute values of the low-frequency limits of the susceptibility spectra are displayed in table 3. We measured only diluted samples ($\phi < 0.005$) to neglect the influence of the particle interactions on the rotational diffusion. The shift of the loss peak due to the viscosity is evident, since the suspensions are prepared from three portions of identical particles dispersed in different suspending media. Toluene has the lowest viscosity with $\eta = 0.55$ mPa s; therefore the loss peak is shifted to higher frequencies. Decane ($\eta = 0.92$ mPa s) and cyclohexane ($\eta = 0.89$ mPa s) have nearly the same viscosity and the loss peaks are in the same regime.

The experimental data demonstrate an increase of the Brownian loss peak as well as a decrease of the real part of the susceptibility for high frequencies by increasing cobalt content. The normalized real part at 250 kHz and the imaginary part of the susceptibility at the maximum of the loss peak are displayed in figure 6. Evidently the real part drops with increasing cobalt content, whereas the imaginary part at the maximum of the loss peak increases. This is experimental evidence for a crossover from Néelian to Brownian relaxation and indicates that for higher cobalt content in the fluid the Néelian relaxation process is increasingly absent. The experimental data are in good agreement with the theoretical prediction.

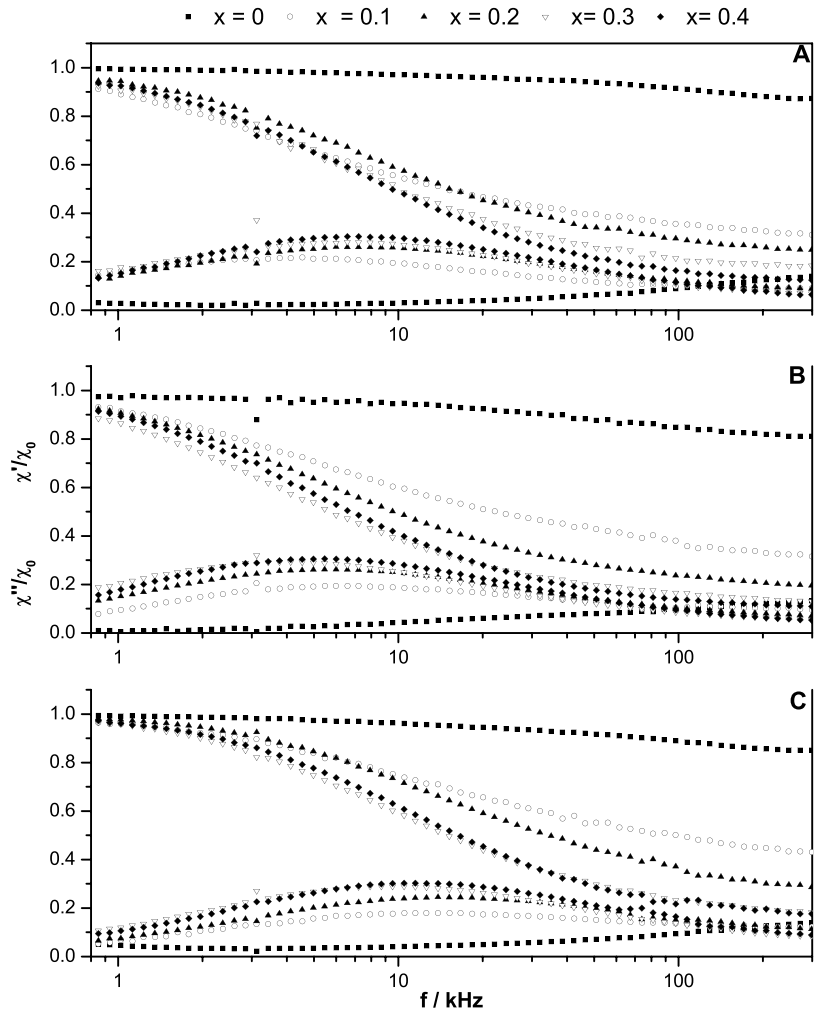

Figure 5. Measured ac-susceptibility for $Co_xFe_{3-x}O_4$ with $x = 0$, 0.1, 0.2, 0.3 and 0.4 in decane (A), cyclohexane (B) and toluene (C).

The predominance of Brownian relaxation can easily be proved by variation of the viscosity of the suspending medium [7].

In figure 7 two least-squares fits of the experimental data according to equation (9) are displayed. For the reason of easier mathematical treatment a Schulz–Flory distribution is used in equation (9) and the data are adapted with a iterative Levenberg–Marquardt algorithm. δ is neglected. The agreement between experimental data and the fit is remarkable in view of the comparatively simple model.

The achieved data are shown in comparison to the data from the DLS in table 4. The diameter measured by the rotational diffusion (ac-χ) of the nanoparticles is slightly smaller than that determined from the translational diffusion (DLS).

5. Conclusion

$Co_xFe_{3-x}O_4$ nanoparticles were prepared by a coprecipitation reaction and stabilized by *N*-methyloleamidoacetic acid as surfactant in three different solvents (toluene, cyclohexane and

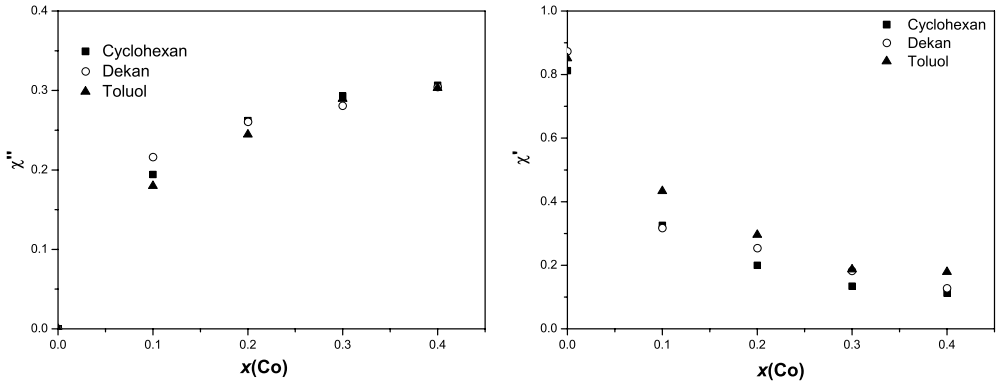

Figure 6. On the left-hand side imaginary part of the normalized susceptibility at the maximum of the loss peak and on the right-hand side the normalized real part of the susceptibility at 250 kHz versus the cobalt content.

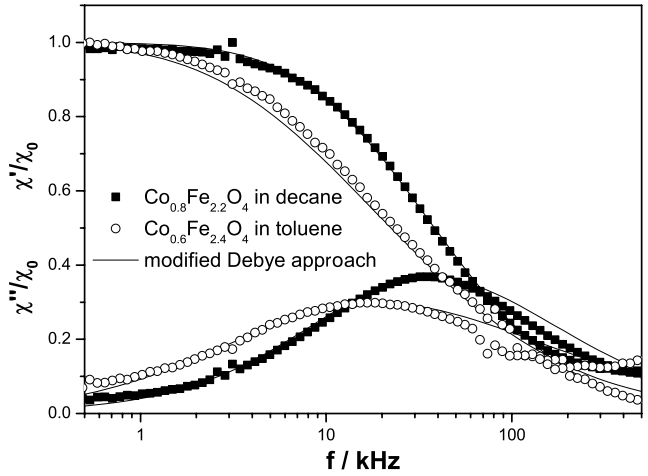

Figure 7. The ac-susceptibility of two samples ($x = 0.8$) in decane and ($x = 0.6$) in toluene and their least-squares fits of the experimental data according to equation (9).

decane). The crystallite size was determined by XRD, whereas the hydrodynamic size was determined by DLS.

The relaxation behaviour, from Néelian to Brownian relaxation process, could gradually be varied by changing the ratio of iron (II) to cobalt (II) salts. For nanoparticles in the range from 5 to 15 nm, a content of cobalt in the order of 10% was sufficient to shift the predominant relaxation mechanism from a Néelian to a Brownian one.

For higher contents of cobalt ($x = 0.5, \ldots, 1$) the ac-susceptibility was measured with a volume fraction ϕ of about 0.005. The achieved diameters were compared to the results from DLS measurements. Again, the diameters determined from the rotational diffusion (from ac-χ) were slightly smaller than those from the translational diffusion coefficient as determined by DLS: the influence of agglomeration on the rotational diffusion is smaller than on the translational diffusion. In contrast to light scattering where the signal is—in the Rayleigh–Debye limit—weighted by the square of the particle volume, in the magnetic susceptibility, the signal is only weighted by the particle volume. As a consequence, scattering experiments

Table 4. Hydrodynamic diameter median and polydispersity as determined by DLS and ac-susceptibility for $Co_xFe_{3-x}O_4$ with $x = 0.5, 0.6, \ldots, 1.0$.

	Toluene				Cyclohexane				Decane			
	ac-χ		DLS		ac-χ		DLS		ac-χ		DLS	
x	D_0 (nm)	P	D_0 (nm)	P	D_0 (nm)	P	D_0 (nm)	P	D_0 (nm)	P	D_0 (nm)	P
0.5	30	0.57	32	0.21	37	0.57	40	0.17	38	0.44	39	0.47
0.6	30	0.50	32	0.22	30	0.21	34	0.23	31	0.52	38	0.85
0.7	23	0.22	23	0.22	29	0.44	33	0.27	31	0.53	24	0.20
0.8	23	0.22	27	0.22	23	0.22	27	0.42	24	0.34	33	0.40
0.9	33	0.41	38	0.37	30	0.41	30	0.27	26	0.23	37	0.34
1.0	25	0.29	31	0.19	27	0.28	29	0.32	27	0.22	32	0.39

are sensitive to the sixth moment of a distribution, whereas magnetization measurements are sensitive to the third moment. For a given non-negligible broadness of a distribution function, the sixth moment has to be larger than the third one. Another reason for the small difference is that by DLS only highly diluted samples could be measured to avoid multiple scattering and absorption. By ac-susceptibility measurements it is important not to have samples of too low concentration. With a magnetic volume fraction ϕ of about 0.005 the influence of the particles interactions to the rotational diffusion can still be neglected. Hence, the hydrodynamic diameter can be calculated from the single-particle Einstein rotational diffusion coefficient.

Acknowledgment

This work has been supported by the DFG Priority Program SPP 1104.

References

[1] Jordan A, Scholz R, Maier-Hauff K, Johannsen M, Wust P, Nadobny J, Schirra H, Schmidt H, Deger S, Loening S, Lanksch W and Felix R 2001 *J. Magn. Magn. Mater.* **225** 118–26
[2] Alexiou C, Jurgons R, Schmid R, Hilpert A, Bergemann C, Parak F and Iro H 2005 *J. Magn. Magn. Mater.* **293** 389–93
[3] Berkovski B and Bashtovoy V 1996 *Magnetic Fluids and Applications Handbook* (New York: Begell House)
[4] Brown W F 1963 *J. Appl. Phys.* **34** 1319–20
[5] See Berkovski B and Bashtovoy V 1996 *Magnetic Fluids and Applications Handbook* (New York: Begell House) p 7
[6] Betancourt-Galindo R, Ayala-Valenzuela O, Garcia-Cerda L A, Rodriguez Fernandez O, Matutes-Aquino J, Ramos G and Yee-Madeira H 2005 *J. Magn. Magn. Mater.* **294** e33–6
[7] Fischer B, Hempelmann R, Lücke R and Huke B 2005 *J. Magn. Magn. Mater.* **289** 74–7
[8] Brown W F 1963 *Phys. Rev.* **130** 1677–86
[9] Neel L 1949 *Ann. Geophys.* **5** 99–136
[10] Kneller E 1963 *Magnetism* vol 3 (New York: Academic) p 382
[11] Shliomis M I 1974 *Sov. Phys.—Usp.* **17** 153–69
[12] Fannin P C and Charles S W 1994 *J. Phys. D: Appl. Phys.* **27** 185–8
[13] Debye P 1929 *Polar Molecules* (New York: Chemical Catalog Company)
[14] Warren B E and Averbach B L 1950 *J. Appl. Phys.* **21** 595–8
Waren B E and Averbach B L 1952 *J. Appl. Phys.* **23** 497
[15] Natter H, Schmelzer M and Hempelmann R 1998 *J. Mater. Res.* **13** 1186–97
[16] Provencher S W 1982 *Comput. Phys. Commun.* **27** 213
Provencher S W 1982 *Comput. Phys. Commun.* **27** 229